# Contrasting roles of clouds as a sink and source of aerosols: a quantitative assessment using WRF-Chem over East Asia

**Young-Hee Ryu, Seung-Ki Min, Christoph Knote**

**Angaben zur Veröffentlichung / Publication details:**

Ryu, Young-Hee, Seung-Ki Min, and Christoph Knote. 2022. "Contrasting roles of clouds as a sink and source of aerosols: a quantitative assessment using WRF-Chem over East Asia." *Atmospheric Environment* 277: 119073. https://doi.org/10.1016/j.atmosenv.2022.119073.

Atmospheric Environment 277 (2022) 119073

Contents lists available at ScienceDirect

Atmospheric Environment

journal homepage: www.elsevier.com/locate/atmosenv

# Contrasting roles of clouds as a sink and source of aerosols: A quantitative assessment using WRF-Chem over East Asia

Young-Hee Ryu [a], Seung-Ki Min [a,c,*], Christoph Knote [b,1]

[a] Division of Environmental Science and Engineering, Pohang University of Science and Technology (POSTECH), Pohang, South Korea
[b] Meteorological Institute, Faculty of Physics, LMU Munich, Munich, Germany
[c] Institute for Convergence Research and Education in Advanced Technology, Yonsei University, Incheon, South Korea

## HIGHLIGHTS

- The effect of wet scavenging by clouds is overall much larger than cloud chemistry.
- But low-level thin clouds have increased chances of forming secondary aerosols.
- The presence of fog increases sulfate formation up to a rate of 1.5 μg $m^{-3}$ $h^{-1}$.

## ARTICLE INFO

*Keywords:*
Cloud
Wet scavenging
Cloud chemistry
Secondary aerosol
WRF-Chem

## ABSTRACT

Clouds play two contrasting roles in the fate of aerosols as a sink through wet scavenging and a source as a medium for aqueous-phase secondary aerosol formation. The contrasting contributions of clouds to near-surface particulate matter with a diameter less than 2.5 μm ($PM_{2.5}$) are quantitatively examined with a particular focus on boundary-layer aerosols and clouds using the Weather Research and Forecasting model coupled with chemistry (WRF-Chem). Overall, the net contribution of wet scavenging to daily-mean $PM_{2.5}$ is much larger (−5 μg $m^{-3}$ to −22 μg $m^{-3}$) than that of cloud chemistry (~0.9 μg $m^{-3}$). The effects of wet scavenging are found over a large spatial extent even over no-rainy regions and last for a long time (~2 days). The amount of aerosols scavenged by clouds and rainfall varies greatly, but it increases as the liquid water path (LWP) increases in a general sense. So, aerosols are mostly removed when clouds have large LWPs. For thin clouds with LWPs of 30–80 g $m^{-2}$, the net reduction in $PM_{2.5}$ due to wet scavenging is barely sensitive to LWP and the role of cloud chemistry becomes non-negligible. A relatively large increase in sulfate mass is found when cloud base height (CBH) is lower than ~1.2 km for thin clouds, and the occurrence fraction in which cloud chemistry plays a dominant role over wet scavenging increases up to ~30% as CBH becomes lower. These results highlight that fog and/or non-precipitating stratus clouds likely play a substantial role in the formation of aqueous-phase secondary aerosols. A case study reveals that the presence of fog can contribute to increasing sulfate formation at a maximum rate of 1.5 μg $m^{-3}$ $h^{-1}$.

## 1. Introduction

It is well known that wet removal by clouds and precipitation is the major sink of aerosols in the atmosphere. Meanwhile, clouds serve as a medium for the formation of secondary aerosols via aqueous-phase chemistry and cloud processing and thus act as a source of aerosols (Ervens, 2015). An increasing number of observational and laboratory studies in recent years have indicated the importance of aqueous-phase chemistry in the formation of sulfate (Ding et al., 2021; Liu et al., 2019) and aqueous secondary organic aerosols (aqSOA) (Lamkaddam et al., 2021; Petters et al., 2021). Overviews of secondary aerosols formed by aqueous-phase chemical reactions and cloud processing are well prescribed in the review articles of Ervens (2015) and McNeill (2015). A recent observational study by Eck et al. (2020) showed that aerosol optical depths and particulate matter with a diameter less than 2.5 μm ($PM_{2.5}$) were increased when clouds and/or fog were present during the

* Corresponding author. 77 Cheongam-ro, Pohang, 37673, South Korea.
*E-mail address:* skmin@postech.ac.kr (S.-K. Min).
[1] Now at: Model-based Environmental Exposure Science, University Augsburg, Augsburg, Germany.

https://doi.org/10.1016/j.atmosenv.2022.119073
Received 1 September 2021; Received in revised form 14 March 2022; Accepted 19 March 2022
Available online 24 March 2022

Korea-United States Air Quality (KORUS-AQ) field campaign over South Korea. Li et al. (2021) found higher mass fractions of secondary inorganic aerosols (sulfate, nitrate, and ammonium) and of SOA during high humidity and fog episodes compared to low humidity periods from another field campaign over the North China Plain (NCP) during 2017–2018. Duan et al. (2021) reported that mass fraction of aqueous-phase-processed oxygenated organic aerosols (aq-OOA) to organic aerosols increased from 2% during non-fog-rain days to 19% during fog-rain days. All these observational studies indicate that secondary inorganic and organic aerosols likely increase when clouds and/or fog are present.

From the perspective of wet scavenging, there have been numerous studies that addressed large influences of wet scavenging by clouds and precipitation on aerosols through theoretical (Bae et al., 2010; Scott, 1982), observational (Emerson et al., 2018; Xu et al., 2019), and modeling (Berg et al., 2015; Croft et al., 2010; Luo et al., 2020) approaches. For example, Bourgeois and Bey (2011) examined the sensitivity of wet scavenging of sulfate and black carbon aerosols to their transport to the Arctic using a global chemistry transport model and showed that wet deposition accounts for 97% and 92% of total deposition of sulfate and black carbon aerosols, respectively. A comprehensive review of wet scavenging by Yang et al. (2019) provides the current understanding and progress of wet scavenging processes for black carbon aerosols.

Previous studies on the roles of clouds in aerosols have focused on one aspect: a sink or a source. A number of studies indicated a negative correlation between sulfate and clouds due to the wet removal of sulfate by clouds (Koch et al., 2003; Plaude et al., 2012; Tai et al., 2010). On the other hand, several studies showed that the in-cloud sulfate formation is the main global sulfate source (>70%) (e.g., Barth et al., 2000; Textor et al., 2006). Yet, few studies have attempted to quantitatively assess such contrasting roles of clouds jointly. It is not well known what kinds of and under which conditions clouds play a dominant role as a sink or a source; how much aerosols can be removed and formed due to clouds; and ultimately what the net effects of clouds are. It is critical to understand and quantify cloud properties because large uncertainties in predicting in-cloud sulfate formation lie in the cloud parameters such as liquid water content, cloud processing time and precipitation rate rather than the in-cloud sulfate formation mechanisms that are quite well established (Ervens, 2015; Pandis and Seinfeld, 1989; Rasch et al., 2000). For a comprehensive understanding of the roles of clouds, we employ the Weather Research and Forecasting model coupled with Chemistry (WRF-Chem) in which wet scavenging processes are recently updated by Ryu and Min (2022). Section 2 describes the numerical experiment setups and observation data used in the model evaluation. The WRF-Chem performance for wet deposition fluxes and surface $PM_{2.5}$ concentration is evaluated in section 3.1. The individual roles of clouds that are examined through sensitivity experiments are quantified and their overall roles are presented and discussed in sections 3.1 through 3.5. Summary and conclusions are made in section 4.

## 2. Experimental design and observation data

### 2.1. WRF-Chem modeling

The WRF-Chem modeling setups in the present study are similar to those used in Ryu et al. (2021), and so only essential parts are described here (the full model configurations are given in Table S1). The study period is from 1 May to 26 May 2016, covering the early period of the KORUS-AQ campaign. All the simulations are initialized at 15 UTC 24 April 2016, and the first six-day results are not used for analysis. Note that the simulations are re-initialized at 15 UTC 23 May 2016 to better capture the meteorology during 24–26 May especially for clouds. The horizontal resolution is 20 km and the ERA-5 reanalysis data are used as initial and boundary conditions for meteorology. For gas and aerosol chemistry, MOZART-4 gas-phase mechanism that was originally developed by Emmons et al. (2010) and updated by Knote et al. (2014) is used with the MOSAIC aerosol module (Zaveri et al., 2008). In the current version of the model, the formation of aqSOA involving cloud/fog water is not explicitly included; however, SOA formation from glyoxal on deliquescent particles is considered (Knote et al., 2014) and wet and dry deposition of gaseous semi-volatile organic compounds is updated by Knote et al. (2015). Thus, the secondary aerosol formation by cloud chemistry and cloud processing mostly aims at the sulfate formation in the present study. For aqueous chemistry, the mechanism of Fahey and Pandis (2001) is used, which includes oxidation of dissolved S(IV) by hydrogen peroxide, ozone, trace metals and radical species in WRF-Chem (Chapman et al., 2009). The pH of cloud droplets is determined by solving the electroneutrality equation using a bisection method, with an assumption that aqueous equilibrium and electroneutrality are continuously maintained (Pandis and Seinfeld, 1989). For aerosol activation the parameterization by Abdul-Razzak and Ghan (2002) is used, which predicts the number and mass fractions of aerosol particles activated for each size section using updraft velocity, aerosol size, number concentration and composition of each size section. It should be noted that considerable updates on wet scavenging processes of aerosols in the MOSAIC module are made by Ryu and Min (2022), and a brief description of the updates can be found in Supplement.

### 2.2. Sensitivity experiments

To investigate the effects of wet scavenging and cloud chemistry separately, we designed four experiments (Table 1). The effect or contribution of each factor can be calculated through Eqs. (1)–(3) according to the factor separation method by Stein and Alpert (1993).

$$\boldsymbol{f}_{wetscav} = \boldsymbol{F}_{wetscav} - \boldsymbol{F}_0, \quad \text{Eq. (1)}$$

$$\boldsymbol{f}_{cldchem} = \boldsymbol{F}_{cldchem} - \boldsymbol{F}_0, \quad \text{Eq. (2)}$$

$$\boldsymbol{f}_{wetscav+cldchem} = \boldsymbol{F}_{control} - \boldsymbol{F}_{wetscav} - \boldsymbol{F}_{cldchem} + \boldsymbol{F}_0, \quad \text{Eq. (3)}$$

where $\boldsymbol{f}_{\text{wetscav}}$, $\boldsymbol{f}_{\text{cldchem}}$, and $\boldsymbol{f}_{\text{wetscav + cldchem}}$ are the contribution of wet scavenging, that of cloud chemistry, and that of the interaction between wet scavenging and cloud chemistry, respectively. The contribution of each factor targets near-surface $PM_{2.5}$ in this study.

### 2.3. Observation data

Three regions are considered for $PM_{2.5}$ evaluation: the Seoul Metropolitan area (hereafter, SMA), the North China Plain (NCP), and the Yangtze River Delta (YRD), which are the most polluted regions within the model domain (see Fig. 3a for the regions). The gridded surface $PM_{2.5}$ data constructed by Ryu and Min (2021) are used for the evaluation over the SMA. These data are constructed based on the routine hourly $PM_{2.5}$ station data (available from https://airkorea.or.kr) using the inverse distance weighted interpolation at $0.25^\circ \times 0.25^\circ$ resolutions. For NCP and YRD regions, the surface reanalysis data at hourly intervals by Kong et al. (2021) are used as pseudo-observations for the model evaluation. The area-averaged daily $PM_{2.5}$ is computed and used for the model evaluation over the three regions. In this study, $PM_{2.5}$ is referred to as near-surface $PM_{2.5}$.

The wet deposition fluxes of soluble inorganic ions, i.e., sulfate ($SO_4^{2-}$), nitrate ($NO_3^-$), and ammonium ($NH_4^+$), measured at the Acid

**Table 1**
List of sensitivity and control experiments.

| Experiment | wet scavenging | cloud chemistry |
|---|---|---|
| $\mathbf{F}_0$ | No | No |
| $\mathbf{F}_{\text{wetscav}}$ | Yes | No |
| $\mathbf{F}_{\text{cldchem}}$ | No | Yes |
| $\mathbf{F}_{\text{control}}$ | Yes | Yes |

Deposition Monitoring Network in East Asia (EANET) stations are utilized in this study (see Fig. S1 for station locations) and the non-sea-salt $SO_4$ flux data are used. The EANET data are available from http s://www.eanet.asia/. Some stations that are located near lakes or over mountains are excluded. The deposition fluxes are summed over the study period (1–26 May 2016), and wet deposition of gaseous species ($SO_2$ for sulfate, $HNO_3$ for nitrate, and $NH_3$ for ammonium) are included in the wet deposition computation with an assumption that the dissolved gas species are ultimately present as ions in raindrops.

The Global Precipitation Measurement (GPM) datasets (Huffman et al., 2017) are utilized and compared to the simulated rainfall over the model domain. The Final Run GPM datasets at hourly intervals and at 0.1° × 0.1° resolutions are used in this study.

## 3. Results and discussion

### 3.1. Evaluation of wet deposition fluxes

To quantitatively examine the role of wet scavenging, a numerical model that reasonably well reproduces wet deposition fluxes is required. The simulated total wet deposition fluxes during the study period are therefore evaluated against the observed fluxes at the EANET stations (Fig. 1). Overall, the model well reproduces nitrate wet deposition flux but underestimates sulfate and ammonium wet deposition fluxes. It has been quite commonly reported that many numerical models underestimate wet deposition fluxes, (e.g., the Model Inter-Comparison Study of Asia (MICS-Asia) phase III reported by Itahashi et al. (2020)). For some stations, the underestimated wet deposition fluxes can be partly

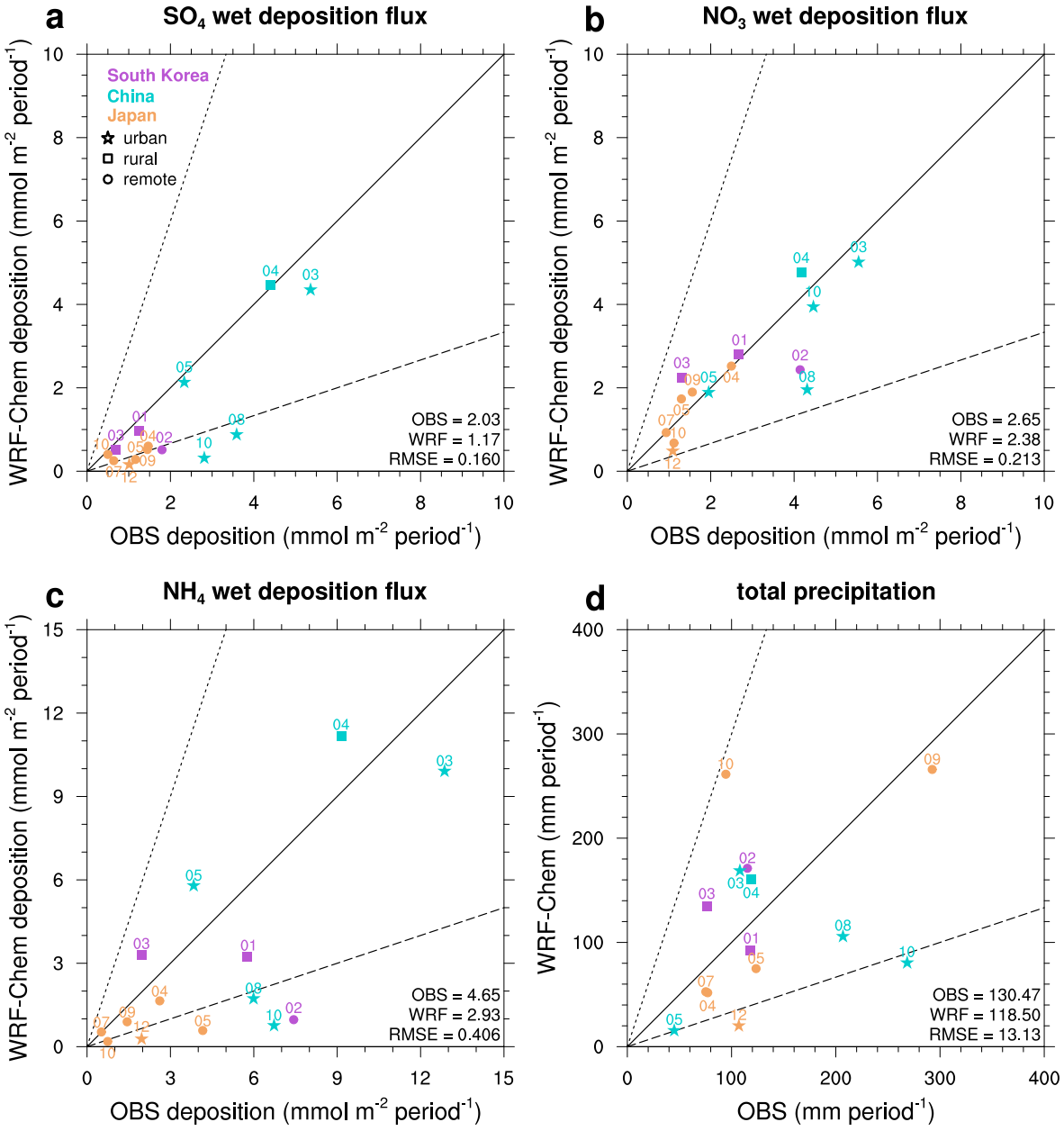


**Fig. 1.** Comparison of total (a) sulfate ($SO_4$), (b) nitrate ($NO_3$), (c) ammonium ($NH_4$) wet deposition fluxes, and (d) precipitation simulated and observed at EANET stations (see Fig. S1 for station locations) during the period of 1–26 May 2016. The OBS, WRF, and RMSE indicate the observation mean, simulation mean, and root-mean-square-error, respectively. The small numbers above or below markers denote the station number with the same color representing countries. The dashed and dotted lines are 3:1 (OBS:WRF) and 1:3 ratio lines, respectively. (For interpretation of the references to color in this figure legend, the reader is referred to the Web version of this article.)

attributed to the underestimated precipitation (e.g., CN08, CN10, and JP12 stations). However, the discrepancies in precipitation do not explain all of the biases in deposition fluxes (e.g., KR02 station). The errors in local emissions and in the transport of gaseous and aerosols are presumably responsible for the errors in deposition fluxes as well. Thus, a more comprehensive comparison of atmospheric concentrations of $SO_4$, $NO_3$, and $NH_4$ with observed ones will be required in the future to see whether the discrepancies are due to the underestimated concentrations or underestimated precipitation or both. Despite the discrepancies, however, the performance of our model simulation is reasonably good as compared to that reported in the MICS-Asia phase III project. For example, in our simulation the normalized mean error (NME) is 42.6% for sulfate, 23.3% for nitrate, and 53.4% for ammonium wet deposition flux, and these are smaller than the NMEs reported in the previous study of Itahashi et al. (2020); the median NME reported in the MICS-Asia phase III project is 67.7% for sulfate, 72.1% for nitrate and 77.7% for ammonium wet deposition flux. Note that the contribution of subgrid-scale wet scavenging by parameterized clouds and precipitation is included in the deposition fluxes but is much smaller than that by resolved clouds and precipitation, which is also shown in Ryu and Min (2022). It is noteworthy that the updated wet scavenging processes improve the model performance by increasing wet deposition fluxes as compared to the previous version. For example, the station-wide averaged wet deposition flux is increased by 17.5% for sulfate, 6.2% for nitrate, and 14.1% for ammonium, leading to closer agreements with the observations (not shown). A detailed analysis comparing the previous and updated version of wet scavenging schemes can be found in Ryu and Min (2022).

### 3.2. Effects of wet scavenging on $PM_{2.5}$

The daily variations of $PM_{2.5}$ from the observations and four experiments are compared in Fig. 2. In the control experiment, daily $PM_{2.5}$ is generally well captured over the three polluted regions except on the days influenced by Asian dust. It is noteworthy that dust loading can be underestimated especially when the GOCART dust emission scheme is used (Zeng et al., 2020) in WRF-Chem. Zeng et al. (2020) and Ryu and Min (2022) also showed the default dry deposition schemes underestimate dust concentration. Even though Ryu and Min (2022) updated dry deposition velocities for coarse-mode particles, the updates are not

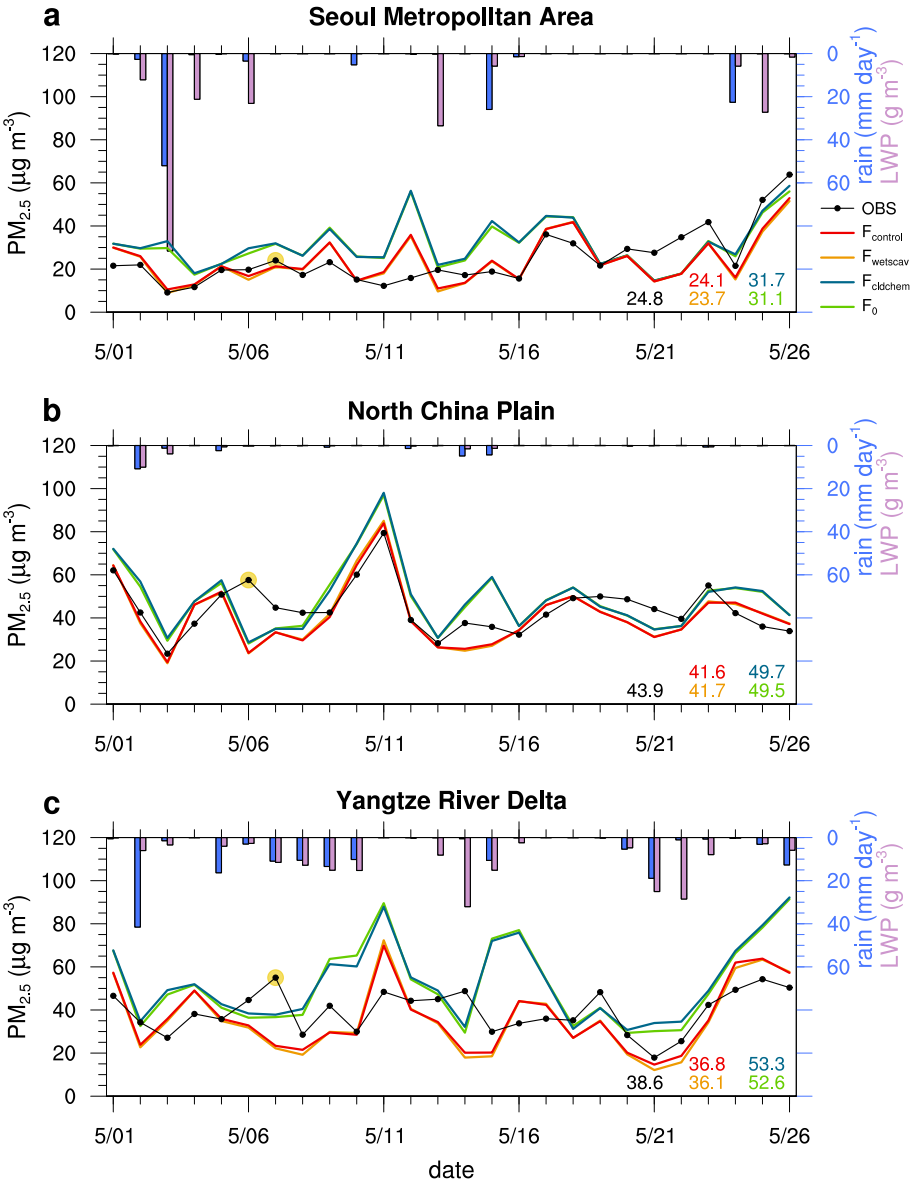


**Fig. 2.** Daily-mean near-surface $PM_{2.5}$ over (a) the Seoul Metropolitan area, (b) North China Plain, and (c) Yangtze River Delta during 1–26 May 2016. The vertical bars on the top of the *x*-axis in light blue and light purple indicate daily-mean rainfall and boundary-layer liquid water path (LWP), respectively, over the three regions. The yellow circles marked on observed $PM_{2.5}$ indicate the days that are influenced by Asian dust. The numbers on the right bottom corner of each subfigure indicate the average $PM_{2.5}$ concentration over the study period, except for Asian dust day, in the same colors representing the individual experiments and observation. (For interpretation of the references to color in this figure legend, the reader is referred to the Web version of this article.)

applied in the present study. It is evident that the contribution of wet scavenging on $PM_{2.5}$ is much larger (cf. $\mathbf{F}_{wetscav}$ and $\mathbf{F}_0$, $\boldsymbol{f}_{wetscav}$ in Eq. (1)) than that of cloud chemistry (cf. $\mathbf{F}_{cldchem}$ and $\mathbf{F}_0$, $\boldsymbol{f}_{cldchem}$ in Eq. (2)). For example, for the SMA, the contribution of wet scavenging is computed as $\mathbf{F}_{wetscav} - \mathbf{F}_0 = 23.7\ \mu g\ m^{-3} - 31.1\ \mu g\ m^{-3} = -7.4\ \mu g\ m^{-3}$. Likewise, the contribution of cloud chemistry is 0.6 μg $m^{-3}$ (= 31.7 μg $m^{-3}$ – 31.1 μg $m^{-3}$). Among the three polluted regions, the effects of wet scavenging are largest over the YRD where frequent and relatively large amounts of rainfall are observed with a maximum contribution of −55 μg $m^{-3}$ for daily $PM_{2.5}$ and −16.5 μg $m^{-3}$ for the study-period average. The effects of wet scavenging (cloud chemistry) relative to the study-period averages in the $\mathbf{F}_0$ experiment are −24% (1.9%) over the SMA, −16% (0.34%) over the NCP, and −31% (1.3%) over the YRD. These values are computed as the ratio of each contribution to the average value in the $\mathbf{F}_0$ experiment; for example, the effect of cloud chemistry over the SMA is $\boldsymbol{f}_{cldchem}/\mathbf{F}_0$ (= 0.6 μg $m^{-3}$/31.1 μg $m^{-3}$ × 100%) and equals to 1.9%. The degree of wet scavenging roughly increases as the amount of rainfall increases (Fig. S2). However, it is not always proportional to the rainfall amounts over that region. For example, the rainfall amount on 2 May over the YRD (41.5 mm) is much larger than that on 10 May (10.2 mm); however, the $\boldsymbol{f}_{wetscav}$ on 2 May (−9.9 μg $m^{-3}$) is much smaller than that on 10 May (−35.9 μg $m^{-3}$). In addition, substantial contributions of wet scavenging are often found even in no-rain days (e.g., 12 May over the SMA and 25 May over the NCP). The reason for this is explained in the next paragraph.

The simulated rainfall amounts as well as distributions are generally in good agreement with the GPM rainfall estimates (Fig. 3a and c). The spatial distributions of rainfall and $\boldsymbol{f}_{wetscav}$ also support that they are not always directly linked. The region exhibiting a large degree of $\boldsymbol{f}_{wetscav}$ over southern China roughly corresponds to the region with large amounts of rainfall. However, the region of the largest $\boldsymbol{f}_{wetscav}$ is shifted to the north of the largest rainfall region, i.e., the region between Sichuan and Chongqing provinces. In addition, the regions with little precipitation (e.g., Henan and Hebei, parts of the NCP) even show remarkable influences of wet scavenging. The reason for this non-trivial relationship is that the amount of aerosols scavenged in the precipitating region (serves as the upwind region) greatly affects the aerosols in the downwind. In other words, if the effects of wet scavenging are ignored, the aerosols that should have been removed by clouds and precipitation are transported to the downwind. So, the effects of wet scavenging can be significant not only in the precipitating region but also in its downwind region. These effects can last a considerably long time (~2 days). Fig. S3 illustrates an example showing that the effects of wet scavenging are accumulated along the pathway of a low-pressure system. The large

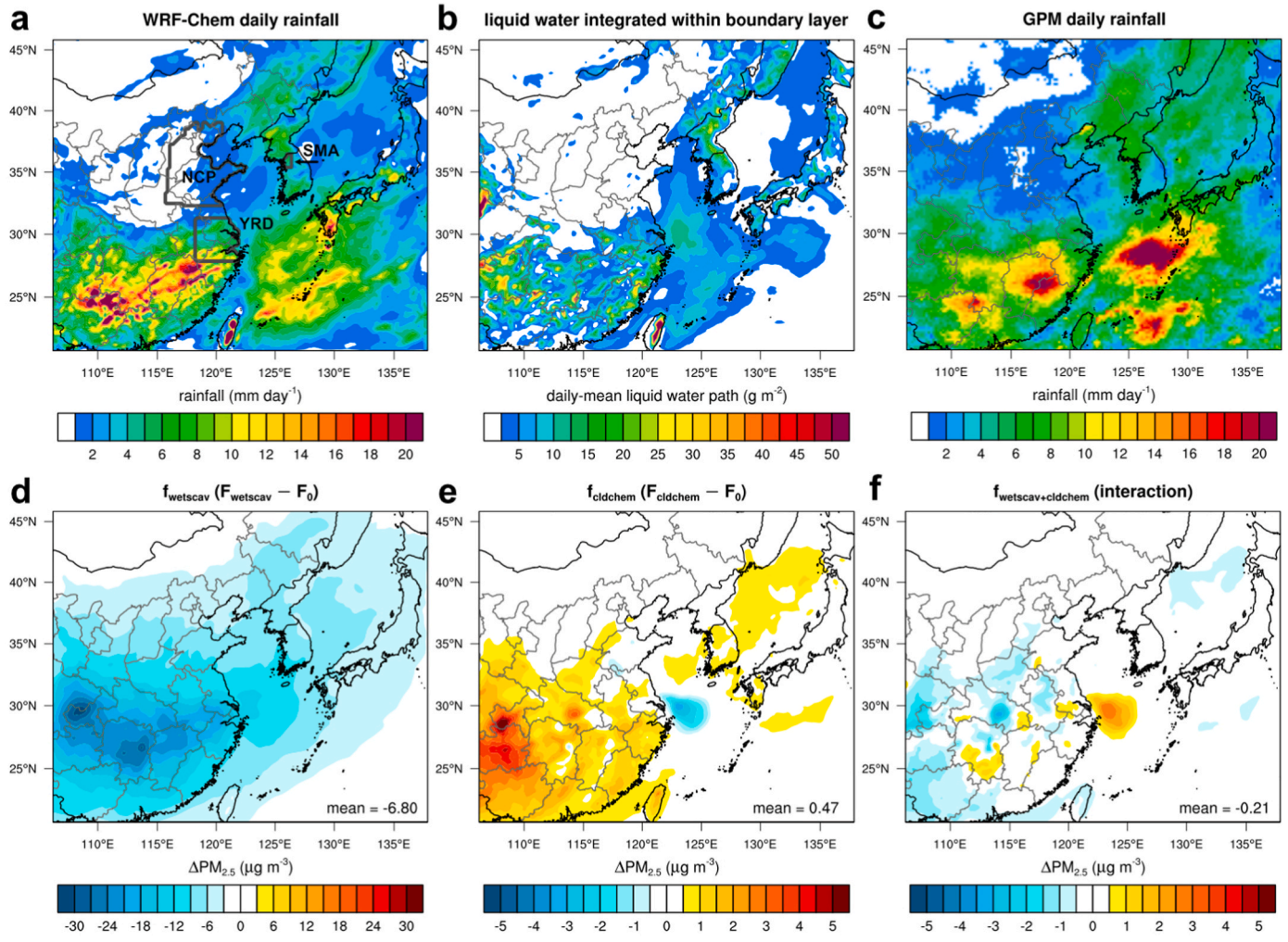


**Fig. 3.** Spatial distributions of (a) rainfall and (b) liquid water path in the $\mathbf{F}_{control}$ experiment, (c) Global Precipitation Measurement (GPM) rainfall, (d) contribution of wet scavenging to near-surface $PM_{2.5}$ computed as a difference between $\mathbf{F}_{wetscav}$ and $\mathbf{F}_0$ experiments ($\mathbf{f}_{wetscav}$), (e) contribution of cloud chemistry computed as a difference between $\mathbf{F}_{cldchem}$ and $\mathbf{F}_0$ experiments ($\mathbf{f}_{cldchem}$), and (f) contribution of the interaction between $f_{wetscav}$ and $\mathbf{f}_{cldchem}$ computed as $\mathbf{F}_{control} - \mathbf{F}_{wetscav} - \mathbf{F}_{cldchem} + \mathbf{F}_0$. All spatial maps shown here are time-averaged ones over the study period of 1–26 May 2016, and the numbers in the right corner in (d)–(f) are the domain-wide averages. Note that the color bar legends in (d) are six timess larger than those in (e) and (f). (For interpretation of the references to color in this figure legend, the reader is referred to the Web version of this article.)

amount of aerosols that should have been scavenged continues to move following the system from mid-north China (15 UTC 13 May), western-to-northeastern China (09 UTC 14 May), southern China (06 UTC 15 May), and finally South Korea (22 UTC 15 May). This is the reason why the effect of wet scavenging is so large on 16 May 2016 without rainfall over the YRD.

It is noteworthy that there are several aspects to be improved or included in the wet scavenging processes in the future, which could serve as some sources of uncertainty in our findings. As an example, cloud-borne (activated) aerosols are assumed to be immediately removed during the in-cloud scavenging processes. That is, such an assumption does not consider the growth of cloud-borne aerosols into larger cloud-borne aerosols and also does not consider their transition to other types of aerosols that are attached to other hydrometers (e.g., rain, ice, graupel, and snow). Because of the immediate wet removal, the resuspension of aerosols from the evaporation of precipitating hydrometeors is not included, which certainly deserves follow-up studies. The multiple evaporations and condensation cycles of aerosols associated with hydrometeors are expected to considerably influence their physical and chemical properties as well as lifetime. Aerosols as ice nuclei are also not treated and so is in-cloud scavenging by solid hydrometeors in the present study, although the wet removal by precipitating snow is included in the below-cloud scavenging process.

### 3.3. Effects of cloud chemistry on $PM_{2.5}$

The effects of cloud chemistry on $PM_{2.5}$ are found to be much smaller than those of wet scavenging with a maximum contribution to daily $PM_{2.5}$ of 3.9 μg $m^{-3}$ over the YRD and with the study-period average of 0.7 μg $m^{-3}$ (Fig. 2c). The spatial distribution of $\boldsymbol{f}_{\mathrm{cldchem}}$ also exhibits its smaller magnitude (Fig. 3e) as compared to that of $\boldsymbol{f}_{\mathrm{wetscav}}$ (Fig. 3d). However, cloud chemistry shows a non-negligible contribution when boundary-layer LWPs are larger than ~20 g $m^{-2}$ (Fig. 2). Note that in Fig. 2 cloud water content is integrated from the surface to the top of the boundary layer, so it is called boundary-layer LWPs. The noticeable contribution of cloud chemistry is found mostly over the YRD where moderate-to-thick clouds with cloud base heights (CBHs) within the boundary layer are often found. The largest contribution of $\boldsymbol{f}_{\mathrm{cldchem}}$ exceeding 5 μg $m^{-3}$ for daily $PM_{2.5}$ is found over Chizhou and Chongqing provinces (Fig. 3e) where clouds with high boundary-layer LWPs are present (Fig. 3b).

The contribution of the interaction between the two factors in Fig. 3f shows overall negative values and their magnitudes are in general smaller (much smaller) than those of cloudy chemistry (wet scavenging). The negative contribution can be interpreted as 1) the wet removal of cloud-borne aerosols that are produced by cloud chemistry and 2) the wet removal of precursors (e.g., $SO_2$, $HNO_3$, and $NH_3$), which in turn reduces in-cloud aerosol formation. The small magnitude of the interaction contribution implies, however, that the contrasting roles of clouds as a source and sink act in a rather independent way. It is worth emphasizing that we examine and compare the sole contributions of the two factors in this study by excluding the contribution of the interaction term. For example, the sole contribution of cloud chemistry is computed as $\mathbf{F_{cldchem}} - \mathbf{F_0}$, and this is different from the control simulation (that includes both factors) minus the simulation without cloud chemistry (i.e., $\mathbf{F_{control}}$–$\mathbf{F_{wetscav}}$). For the SMA, the sole contribution of cloud chemistry is 0.6 μg $m^{-3}$ (= $\mathbf{F_{cldchem}} - \mathbf{F_0}$), and this is smaller than the value computed as $\mathbf{F_{control}} - \mathbf{F_{wetscav}}$ ($= \boldsymbol{f}_{\mathrm{cldchem}} + \boldsymbol{f}_{\mathrm{wetscav\ +\ cldchem}} = 0.4$ μg $m^{-3}$). The former does not include the interaction term, but the latter does. There are other ways to quantify individual contributions of factors, for example, linear-sum, shared-interaction, and scaled-residual factorizations (Lunt et al., 2021). These factorizations do not explicitly represent interaction terms between factors; rather, contributions of interactions are shared and distributed to contributions of individual factors (see Lunt et al., 2021 for details). Because the interaction between wet scavenging and cloud chemistry is found to be small in this study, our conclusions would not change if other factorization methods are applied.

### 3.4. Overall effects of clouds

Because the effects of wet scavenging and cloud chemistry are opposite and thus act to cancel each other out, the net changes in $PM_{2.5}$ and sulfate aerosol due to wet scavenging and cloud chemistry are examined with respect to LWPs or CBHs (Fig. 4). The net change is computed as the difference in aerosol concentration between $\mathbf{F}_{\mathrm{control}}$ and $\mathbf{F}_0$ ($= \boldsymbol{f}_{\mathrm{wetscav}} + \boldsymbol{f}_{\mathrm{cldchem}} + \boldsymbol{f}_{\mathrm{wetscav\ +\ cldchem}}$). So, a net positive (negative) change means that the effects of cloud chemistry (wet scavenging) play a dominant role and overcome the opposite contribution of the other factor and that of their interaction. Here, the LWPs are total column LWPs because these LWPs are more representative of LWPs for precipitating clouds and thus more appropriate to examine the contribution of wet scavenging. The extremely scattered distribution of net negative changes in $PM_{2.5}$ with respect to LWPs in Fig. 4a indicates that the effects of wet scavenging are very variable. The distribution of net change in $PM_{2.5}$ in a given LWP bin is positively skewed in terms of magnitude, and so the median values are closer to the 25th percentile values than to the 75th percentile values. Such characteristics are also found in the distributions of the net change in sulfate with respect to LWP (Fig. 4b) and to CBH (Fig. 4c). The median values and interquartile ranges for net positive changes in $PM_{2.5}$ and sulfate are shown in Fig. S4. The degree of wet scavenging measured by the median values generally increases as LWP increases from −5 μg $m^{-3}$ (on average when LWPs are less than 10 g $m^{-2}$) to −22 μg $m^{-3}$ (when LWPs are greater than 360 g $m^{-2}$). On the other hand, the median values of net positive changes do not significantly increase with LWPs once LWP is greater than 30 g $m^{-2}$, showing about 0.9 μg $m^{-3}$. Such a weak sensitivity of cloud-borne aerosols to the amounts of cloud water was also found by Ervens et al. (2008), and they showed that the in-cloud aerosol formation is less sensitive to cloud liquid water content than to cloud-contact time.

Interestingly, the median values of net negative changes barely increase in magnitude when LWP ranges from 30 to 80 g $m^{-2}$ (the plateau seen in the median line in Fig. 4a). Additionally, we present the occurrence fraction that is the ratio of the number of samples in which cloud chemistry plays a dominant role in $PM_{2.5}$ changes (so the net change becomes positive) relative to the total number of samples in a given LWP range (the purple dashed line in Fig. 4a). For example, when the LWPs are 32–36 g $m^{-2}$ the total number of samples is 3978 in the bin; the number of samples that have net positive changes in $PM_{2.5}$ is 334; and this means that a fraction of 8.4% (= 334/3978) among the total samples gains mass due to clouds. At the same time, this indicates that the fraction of about 92% among the total samples experiences a net mass loss due to clouds because the effects of wet scavenging are dominant over those of cloud chemistry. Overall, the fraction in which wet scavenging plays a dominant role is always much larger than that of cloud chemistry. However, for LWPs of 30–80 g $m^{-2}$ the fraction in which the effects of cloud chemistry surpass those of wet scavenging can be non-negligible. This suggests that when clouds with low LWPs (30–80 g $m^{-2}$) are present, which are highly likely non-precipitating clouds due to their low LWPs, the cloud chemistry has enhanced chances to increase $PM_{2.5}$ mass with a maximum occurrence fraction of about 8–9%. However, for clouds with moderate-to-high LWPs, the contribution of wet scavenging is much greater than that of cloud chemistry and the majority of the samples show net mass losses.

Because the increase in aerosol mass due to cloud chemistry is mostly confined to sulfate aerosol in the present study, the net change in sulfate aerosol is also examined (Fig. 4b). Similar to $PM_{2.5}$, the fraction in which cloud chemistry plays a dominant role is relatively high when LWPs are smaller about 80 g $m^{-2}$ with a maximum value of 17%. For sulfate, the median values of net negative change are smaller than for those for $PM_{2.5}$ (e.g., about −3 μg $m^{-3}$ for sulfate versus −22 μg $m^{-3}$ for $PM_{2.5}$ with LWPs of 380–440 g $m^{-2}$). In other words, the contribution of wet

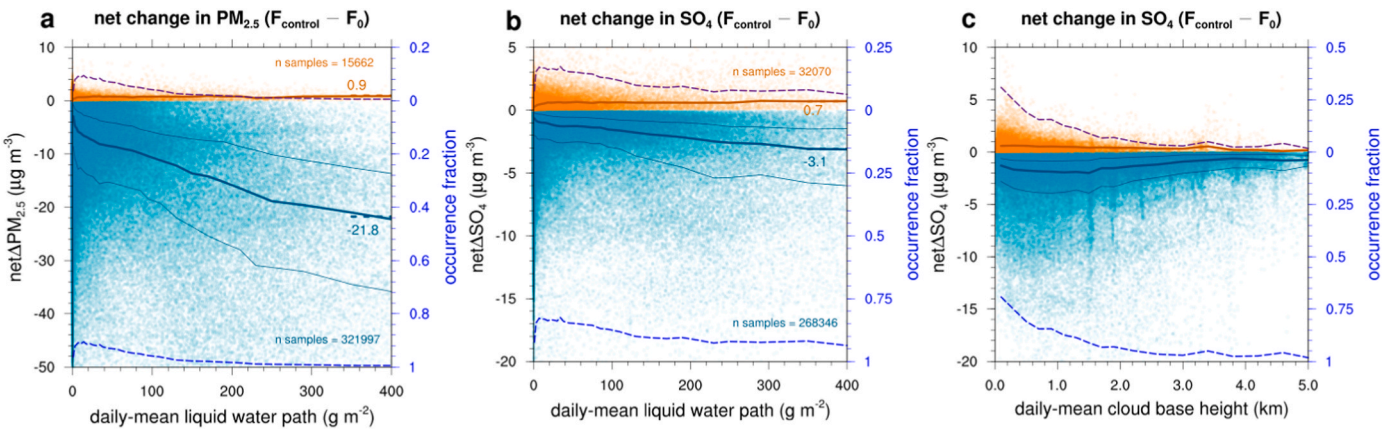


**Fig. 4.** (a) Scatter plot of the net change in near-surface daily $PM_{2.5}$ ($\mathbf{F}_{control} - \mathbf{F}_0$) with respect to daily-mean liquid water path (LWP) at all land grids. The thick solid lines in dark orange (cyan) are the median values of net positive (negative) change in $PM_{2.5}$ in a given LWP bin. The thin-cyan solid lines indicate the lower and upper interquartiles (25th and 75th percentiles) for net negative change in $PM_{2.5}$. The LWP bins are at intervals of 2 g $m^{-2}$ when LWPs are up to 8 g $m^{-2}$, 4 g $m^{-2}$ for LWPs of 12–36 g $m^{-2}$, 10 g $m^{-2}$ for LWPs of 40–100 g $m^{-2}$, 20 g $m^{-2}$ for LWPs of 120–260 g $m^{-2}$, and 60 g $m^{-2}$ when LWPs are greater than or equal to 320 g $m^{-2}$. The dashed lines in purple (blue) indicate the occurrence fraction of net positive (negative) change in $PM_{2.5}$ for a given LWP bin. Read the right *y*-axis for the fraction values. (b) is the same for (a), but for sulfate ($SO_4$) aerosols with a diameter less than 2.5 μm. (c) is the same for (b), but with respect to daily-mean cloud base height. The intervals of cloud base height are 200 m. Note that only land grids in which the absolute magnitude of the net change in $PM_{2.5}$ is greater than 0.1 μg $m^{-3}$ and that in $SO_4$ greater than 0.05 μg $m^{-3}$ are considered. (For interpretation of the references to color in this figure legend, the reader is referred to the Web version of this article.)

scavenging is much larger for $PM_{2.5}$ than sulfate. This is because the individual species of $PM_{2.5}$ other than sulfate barely undergo cloud chemistry/processing in the current version of the model, so those species experience almost wet scavenging only. These results underscore a greater potential of cloud chemistry to secondary aerosol formation if additional mechanisms such as aqSOA formation are included in the model. Even though additional mechanisms are considered, however, the conclusions drawn in this study would not change and conclusions with additional mechanisms are expected to be similar to those drawn for sulfate aerosols. That is, cloud chemistry would have increased chances of increasing secondary aerosol mass when LWP is low (30–80 g $m^{-2}$) but its role would become much smaller than the role of wet scavenging as LWP increases.

The contribution of cloud chemistry to sulfate formation shows a meaningful link to CBH (Fig. 4c). The fraction that shows dominant contributions of cloud chemistry increases up to 30.8% as CBH decreases particularly for CBHs lower than ~1.2 km. The maximum median value of net positive contribution for sulfate is 0.62 μg $m^{-3}$ when CBHs range from 0.2 to 0.4 km. On the other hand, the relationship between CBH and net negative contribution is less clear. The median values of net negative changes range from −1.3 μg $m^{-3}$ to −2.0 μg $m^{-3}$ when CBHs are lower than 1.6 km, and decrease in magnitude as CBH increases. Thus, sizable sulfate formation by cloud chemistry can be expected when clouds have a low base height within the boundary layer. Considering the growing negative contribution of wet scavenging with increasing LWPs, the occurrence fraction that shows enhanced $PM_{2.5}$ mass due to cloud chemistry would become relatively high when the LWPs of clouds range from 30 to 80 g $m^{-2}$ and their base heights are close to the surface. These cases correspond to fog or non-precipitating stratus clouds. It is worth noting that LWPs for fog typically range from 20 to 100 g $m^{-2}$ (Dupont et al., 2018; Gultepe et al., 2009). The clouds with low CBHs indeed serve as an ideal medium for secondary aerosol formation because considerable amounts of precursors (e.g., $SO_2$) can be transported upward from the boundary layer to the clouds.

### 3.5. Case study during 24–26 May KORUS campaign period

High $PM_{2.5}$ concentrations were observed during 25–26 May over the SMA (Fig. 2a). According to Peterson et al. (2019), the increase in $PM_{2.5}$ concentration over the SMA during this period is attributed to the transboundary transport of pollutants from China. The hourly time series of observed $PM_{2.5}$ clearly shows its increasing concentration after a cold front passage (after 09 local time on 24 May) (Fig. 5a). The model reasonably well reproduces the timing of the cold front passage and the low $PM_{2.5}$ concentration while rainfalls were recorded (06–09 local time). The contribution of wet scavenging reaches a peak during the cold front passage, which reduces hourly $PM_{2.5}$ by up to 23 μg $m^{-3}$ (Fig. 5b). Similar to the example shown in Fig. S3, the significant effects of wet scavenging last for ~1.5 days (from 06 local time on 24 May up to 18 local time on 25 May) even though the rainfall duration is short (~6 h).

The contribution of cloud chemistry is found to be largest for sulfate followed by ammonium aerosols as expected (Fig. 5c). The largest rate of sulfate formation by cloud chemistry is about 1 μg $m^{-3}$ $h^{-1}$ on 24 May. This is in line with the missing sulfate formation with rates of 0.3–5 μg $m^{-3}$ $h^{-1}$ from model simulations for severe haze events in Beijing in January 2013 (Liu et al., 2020; Zheng et al., 2015). The sulfate formation rate during the later period (e.g., nighttime hours on 25–26 May) is rather lower than that on 24 May. However, this can be significantly high locally near clouds/fog (up to 1.5 μg $m^{-3}$ $h^{-1}$, Fig. 6i). In fact, the higher sulfate formation rate on 24 May is likely due to the clouds with the large horizontal extent that covers entire South Korea (i.e., a cold front with the horizontal extent of 300–400 km). The clouds/fog simulated on 25 and 26 May are rather small, and the SMA is only partially covered by the clouds/fogs (Fig. 6). Note that the clouds simulated during nighttime on 25 and 26 May can be classified as a fog because their depths are shallow and base heights are near the surface (not shown). In Fig. 6g–i, the large sulfate formation is found near the southern edge of the clouds where $SO_2$ concentration and LWPs are both moderately high, suggesting the necessity of co-location of precursors and clouds. Thus, during the transboundary transport that brought a significant amount of pollutants, the presence of non-precipitating low-level clouds/fog plays a substantial role in increasing sulfate concentration with a maximum rate of 1.5 μg $m^{-3}$ $h^{-1}$.

As shown in Fig. 3f, the contribution of the interaction between the two factors is found to be generally small (Fig. 5d). We showed our model's reasonable capability of simulating wet deposition fluxes (Fig. 1) and surface $PM_{2.5}$ (Fig. 2). Nonetheless, the near-surface $PM_{2.5}$ over the SMA is underestimated during 25–26 May (Fig. 5a). Tsui et al. (2019) showed that the formation rate of isoprene epoxydiol SOA is ~0.4 μg $m^{-3}$ $h^{-1}$ for cloud droplet pH of 4. Ervens et al. (2011)

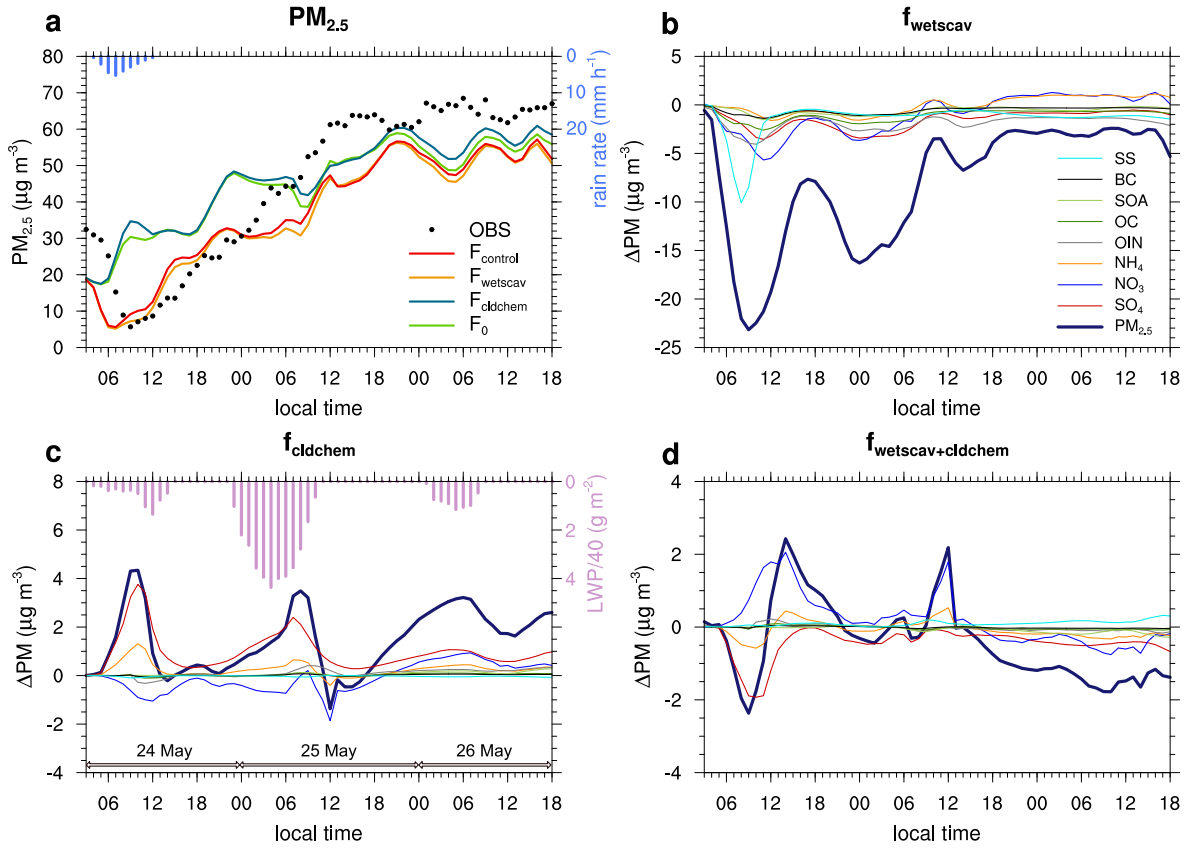


**Fig. 5.** (a) Hourly time series of $PM_{2.5}$ from surface observations over the Seoul Metropolitan area (SMA) and from the four WRF-Chem experiments during 24–26 May 2016. The observed $PM_{2.5}$ values at multiple sites in the SMA are averaged. The blue bars on the top *x*-axis indicate the hourly rain rate over the SMA in the control experiment ($\mathbf{F}_{control}$). (b) Hourly time series of the contribution of wet scavenging to $PM_{2.5}$ and its chemical composition. In the legend, SS is the sea salt, BC is the black carbon, OC is the organic carbon, and OIN is the other inorganic aerosols. (c) Same as in (b), but for the contribution of cloud chemistry. The pink bars on the top *x*-axis in (c) are the liquid water paths integrated within the boundary layer. (d) Same as in (b), but for the contribution of the interaction between wet scavenging and cloud chemistry. (For interpretation of the references to color in this figure legend, the reader is referred to the Web version of this article.)

demonstrated that about 1 μg $m^{-3}$ of aqSOA (sum of oxalic, glyoxylic, glycolic, and pyruvic acid masses) remains after a 4-h simulation of cloud processing and evaporation, yielding a roughly 0.25 μg $m^{-3}$ $h^{-1}$ formation rate. A regional-scale modeling study of Fahey et al. (2017) showed that the inclusion of aqSOA formation from biogenic epoxides increases surface $PM_{2.5}$ concentration over the eastern US with a maximum increase in the monthly mean value of ~20 ng $m^{-3}$. It is doubtless that including aqSOA formation will resolve at least partially the discrepancies between observed and simulated $PM_{2.5}$. Given that the formation rates of aqSOA are lower than or comparable to that of sulfate aerosol, however, more attention should be paid to under-/-mis-representation of clouds in terms of location, duration, horizontal extent, and LWP.

## 4. Summary and conclusions

The WRF-Chem modeling in this study shows a satisfactory performance in reproducing near-surface $PM_{2.5}$ as well as wet deposition fluxes over East Asia. Overall, the negative role of clouds as a sink of aerosols is more dominant than their positive role as a source of aerosols. For example, the sole contribution of wet scavenging to daily mean $PM_{2.5}$ is up to −55 μg $m^{-3}$ over the YRD, while the maximum contribution of cloud chemistry is about 4 μg $m^{-3}$. These are the sole contributions of individual roles and so when these two are considered together, the net effect of clouds becomes smaller than those of individual roles. The contribution of the interaction between the two factors is smaller than those of the two factors. For domain-wide averages, the net negative contribution of wet scavenging to daily $PM_{2.5}$ with respect to LWPs ranges from −5 μg $m^{-3}$ to −22 μg $m^{-3}$ and the positive one of cloud chemistry is about 0.9 μg $m^{-3}$. The degree of wet scavenging is very variable, and the effects of wet scavenging are found over a large spatial extent even over non-precipitating regions and for a long duration (~2 days). This is because the amount of wet scavenging depends not only on rainfall amounts or LWPs but also on aerosol concentrations along with the footprint of cloud systems. Although the contribution of cloud chemistry is small compared to that of wet scavenging in a general sense, an increase in the probability of which cloud chemistry plays a dominant role over wet scavenging is found when low-level clouds/fog with low LWPs of 30–80 g $m^{-2}$ are present (at least their base heights are within boundary layer). For sulfate aerosol, the maximum probability of which the effects of cloud chemistry surpass those of wet scavenging thus resulting in increases in sulfate mass is about 17%. In other words, in the presence of low-level thin clouds or fog we can expect increases in sulfate mass in roughly 1 out of 5 cases. The SMA episode also confirms the larger contribution of wet scavenging than cloud chemistry during the rainfall period and up to ~1.5 days after rainfall. After the effects of wet scavenging phase out, the presence of low-level clouds/fog over the SMA is found to increase sulfate formation at a maximum rate of 1.5 μg $m^{-3}$ $h^{-1}$. As aqSOA formation mechanisms are not explicitly included in the current version of the model, the effects of aqSOA formation on aerosols deserve a follow-up study and are expected to increase secondary aerosol concentrations when low-level clouds/fog are present.

## CRediT authorship contribution statement

**Young-Hee Ryu:** Formal analysis, Methodology, Data curation,

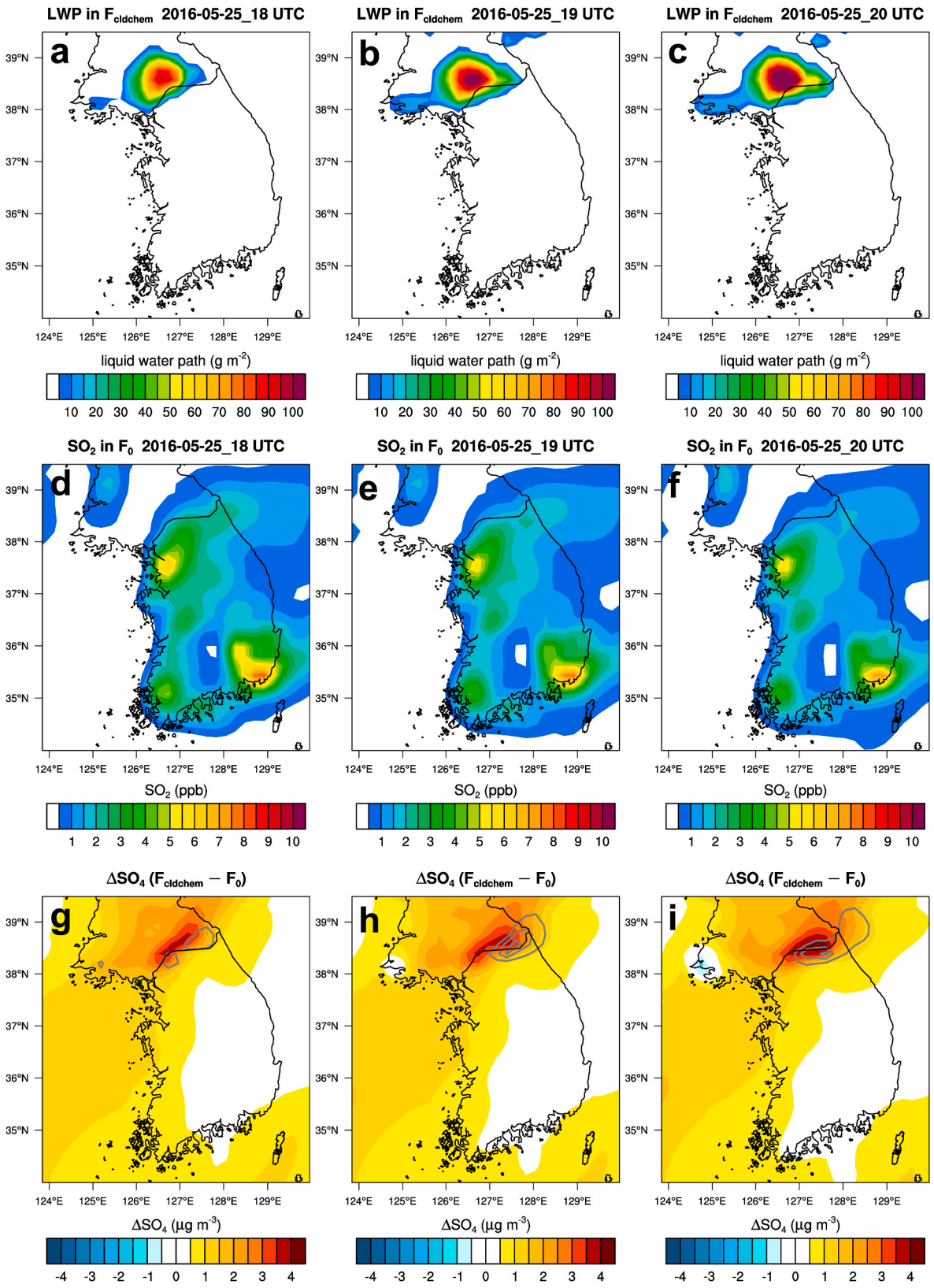


**Fig. 6.** Liquid water path (LWP) in the $\mathbf{F}_{\text{cldchem}}$ experiment (a) at 18 UTC 25 May 2016, (b) 19 UTC 25 May 2016, and (c) at 20 UTC 25 May 2016. (d–f) Near-surface $SO_2$ concentration in the $\mathbf{F}_0$ experiment at the same times shown in (a–c), respectively. (g–i) Difference in sulfate aerosol concentration with a diameter less than 2.5 μm between $\mathbf{F}_{\text{cldchem}}$ and $\mathbf{F}_0$ experiments at the same times shown in (a–c), respectively. The gray contours indicate the difference in sulfate concentration in an hour; for example, the contours in (g) indicate the sulfate concentrations at 18 UTC minus those at 17 UTC. The levels of the contours are 0.5, 1.0, and 1.5 μg $m^{-3}$ $h^{-1}$.

Visualization, Writing. **Seung-Ki Min:** Conceptualization, Supervision, Funding acquisition, Writing – review & editing. **Christoph Knote:** Methodology, Model development, Writing – review & editing.

## Declaration of competing interest

The authors declare that they have no known competing financial interests or personal relationships that could have appeared to influence the work reported in this paper.

## Acknowledgment

The authors would like to thank three anonymous reviewers for their insightful and constructive comments, which helped us improve this article. This study is supported by the Korea Meteorological Administration Research and Development Program under Grant KMI2020-01413.

## Appendix A. Supplementary data

Supplementary data to this article can be found online at https://doi.org/10.1016/j.atmosenv.2022.119073.

## References

Abdul-Razzak, H., Ghan, S.J., 2002. A parameterization of aerosol activation 3. Sectional representation. J. Geophys. Res. Atmos. 107 https://doi.org/10.1029/2001JD000483. AAC 1-1-AAC 1-6.

Bae, S.Y., Jung, C.H., Kim, Y.P., 2010. Derivation and verification of an aerosol dynamics expression for the below-cloud scavenging process using the moment method. J. Aerosol Sci. 41, 266–280. https://doi.org/10.1016/j.jaerosci.2009.11.006.

Barth, M.C., Rasch, P.J., Kiehl, J.T., Benkovitz, C.M., Schwartz, S.E., 2000. Sulfur chemistry in the National Center for atmospheric Research Community climate model: description, evaluation, features, and sensitivity to aqueous chemistry. J. Geophys. Res. Atmos. 105, 1387–1415. https://doi.org/10.1029/1999JD900773.

Berg, L.K., Shrivastava, M., Easter, R.C., Fast, J.D., Chapman, E.G., Liu, Y., Ferrare, R.A., 2015. A new WRF-Chem treatment for studying regional-scale impacts of cloud processes on aerosol and trace gases in parameterized cumuli. Geosci. Model Dev. (GMD) 8, 409–429. https://doi.org/10.5194/gmd-8-409-2015.

Bourgeois, Q., Bey, I., 2011. Pollution transport efficiency toward the Arctic: sensitivity to aerosol scavenging and source regions. J. Geophys. Res. Atmos. 116 https://doi.org/10.1029/2010JD015096.

Chapman, E.G., Gustafson, W.I.J., Easter, R.C., Barnard, J.C., Ghan, S.J., Pekour, M.S., Fast, J.D., 2009. Coupling aerosol-cloud-radiative processes in the WRF-Chem model: investigating the radiative impact of elevated point sources. Atmos. Chem. Phys. 9, 945–964. https://doi.org/10.5194/acp-9-945-2009.

Croft, B., Lohmann, U., Martin, R.V., Stier, P., Wurzler, S., Feichter, J., Hoose, C., Heikkilä, U., van Donkelaar, A., Ferrachat, S., 2010. Influences of in-cloud aerosol scavenging parameterizations on aerosol concentrations and wet deposition in ECHAM5-HAM. Atmos. Chem. Phys. 10, 1511–1543. https://doi.org/10.5194/acp-10-1511-2010.

Ding, X., Li, Q., Wu, D., Wang, X., Li, M., Wang, T., Wang, L., Chen, J., 2021. Direct observation of sulfate explosive growth in wet plumes emitted from typical Coal-fired stationary sources. Geophys. Res. Lett. 48, e2020GL092071 https://doi.org/10.1029/2020GL092071.

Duan, J., Huang, R.-J., Gu, Y., Lin, C., Zhong, H., Wang, Y., Yuan, W., Ni, H., Yang, L., Chen, Y., Worsnop, D.R., O'Dowd, C., 2021. The formation and evolution of secondary organic aerosol during summer in Xi'an: aqueous phase processing in fog-rain days. Sci. Total Environ. 756, 144077. https://doi.org/10.1016/j.scitotenv.2020.144077.

Dupont, J.-C., Haeffelin, M., Wærsted, E., Delanoe, J., Renard, J.-B., Preissler, J., O'Dowd, C., 2018. Evaluation of fog and low stratus cloud microphysical properties derived from in situ sensor, cloud radar and SYRSOC algorithm. Atmosphere 9, 169. https://doi.org/10.3390/atmos9050169.

Eck, T.F., Holben, B.N., Kim, J., Beyersdorf, A.J., Choi, M., Lee, S., Koo, J.-H., Giles, D.M., Schafer, J.S., Sinyuk, A., Peterson, D.A., Reid, J.S., Arola, A., Slutsker, I., Smirnov, A., Sorokin, M., Kraft, J., Crawford, J.H., Anderson, B.E., Thornhill, K.L., Diskin, G., Kim, S.-W., Park, S., 2020. Influence of cloud, fog, and high relative humidity during pollution transport events in South Korea: aerosol properties and PM2.5 variability. Atmos. Environ. 232, 117530. https://doi.org/10.1016/j.atmosenv.2020.117530.

Emerson, E.W., Katich, J.M., Schwarz, J.P., McMeeking, G.R., Farmer, D.K., 2018. Direct measurements of dry and wet deposition of black carbon over a Grassland. J. Geophys. Res. Atmos. 123 (12) https://doi.org/10.1029/2018JD028954, 277-12,290.

Emmons, L.K., Walters, S., Hess, P.G., Lamarque, J.-F., Pfister, G.G., Fillmore, D., Granier, C., Guenther, A., Kinnison, D., Laepple, T., Orlando, J., Tie, X., Tyndall, G., Wiedinmyer, C., Baughcum, S.L., Kloster, S., 2010. Description and evaluation of the model for ozone and related chemical Tracers, version 4 (MOZART-4). Geosci. Model Dev. 3, 43–67. https://doi.org/10.5194/gmd-3-43-2010.

Ervens, B., 2015. Modeling the processing of aerosol and trace gases in clouds and fogs. Chem. Rev. 115, 4157–4198. https://doi.org/10.1021/cr5005887.

Ervens, B., Carlton, A.G., Turpin, B.J., Altieri, K.E., Kreidenweis, S.M., Feingold, G., 2008. Secondary organic aerosol yields from cloud-processing of isoprene oxidation products. Geophys. Res. Lett. 35 https://doi.org/10.1029/2007GL031828.

Ervens, B., Turpin, B.J., Weber, R.J., 2011. Secondary organic aerosol formation in cloud droplets and aqueous particles (aqSOA): a review of laboratory, field and model studies. Atmos. Chem. Phys. 11, 11069–11102. https://doi.org/10.5194/acp-11-11069-2011.

Fahey, K.M., Carlton, A.G., Pye, H.O.T., Baek, J., Hutzell, W.T., Stanier, C.O., Baker, K.R., Appel, K.W., Jaoui, M., Offenberg, J.H., 2017. A framework for expanding aqueous chemistry in the Community Multiscale Air Quality (CMAQ) model version 5.1. Geoscientific Model. Development 10, 1587–1605. https://doi.org/10.5194/gmd-10-1587-2017.

Fahey, K.M., Pandis, S.N., 2001. Optimizing model performance: variable size resolution in cloud chemistry modeling. Atmos. Environ. 35, 4471–4478. https://doi.org/10.1016/S1352-2310(01)00224-2.

Gultepe, I., Pearson, G., Milbrandt, J.A., Hansen, B., Platnick, S., Taylor, P., Gordon, M., Oakley, J.P., Cober, S.G., 2009. The fog remote sensing and modeling field project. Bull. Am. Meteorol. Soc. 90, 341–360. https://doi.org/10.1175/2008BAMS2354.1.

Huffman, G.J., Bolvin, D.T., Braithwaite, D., Hsu, K., Joyce, R., Kidd, C., Nelkin, E.J., Sorooshian, S., Tan, J. and Xie, P. (2017) Algorithm theoretical basis document (ATBD) version 4.6 for the NASA Global Precipitation Measurement (GPM) Integrated Multi-satellitE Retrievals for GPM (IMERG). 32 pp. Greenbelt, MD: GPM Project. Available at: https://pmm.nasa.gov/sites/default/files/document_files/IMERG_ATBD_V4.6.pdf [Accessed 12th January 2021].

Itahashi, S., Ge, B., Sato, K., Fu, J.S., Wang, X., Yamaji, K., Nagashima, T., Li, J., Kajino, M., Liao, H., Zhang, M., Wang, Zhe, Li, M., Kurokawa, J., Carmichael, G.R., Wang, Zifa, 2020. MICS-Asia III: overview of model intercomparison and evaluation of acid deposition over Asia. Atmos. Chem. Phys. 20, 2667–2693. https://doi.org/10.5194/acp-20-2667-2020.

Knote, C., Hodzic, A., Jimenez, J.L., 2015. The effect of dry and wet deposition of condensable vapors on secondary organic aerosols concentrations over the continental US. Atmos. Chem. Phys. 15, 1–18. https://doi.org/10.5194/acp-15-1-2015.

Knote, C., Hodzic, A., Jimenez, J.L., Volkamer, R., Orlando, J.J., Baidar, S., Brioude, J., Fast, J., Gentner, D.R., Goldstein, A.H., Hayes, P.L., Knighton, W.B., Oetjen, H., Setyan, A., Stark, H., Thalman, R., Tyndall, G., Washenfelder, R., Waxman, E., Zhang, Q., 2014. Simulation of semi-explicit mechanisms of SOA formation from glyoxal in aerosol in a 3-D model. Atmos. Chem. Phys. 14, 6213–6239. https://doi.org/10.5194/acp-14-6213-2014.

Koch, D., Park, J., Del Genio, A., 2003. Clouds and sulfate are anticorrelated: a new diagnostic for global sulfur models. J. Geophys. Res. Atmos. 108 https://doi.org/10.1029/2003JD003621.

Kong, L., Tang, X., Zhu, J., Wang, Z., Li, J., Wu, H., Wu, Q., Chen, H., Zhu, L., Wang, W., Liu, B., Wang, Q., Chen, D., Pan, Y., Song, T., Li, F., Zheng, H., Jia, G., Lu, M., Wu, L., Carmichael, G.R., 2021. A six-year long (2013–2018) high-resolution air quality reanalysis dataset over China base on the assimilation of surface observations from CNEMC. Earth Syst. Sci. Data 13, 529–570. https://doi.org/10.5194/essd-13-529-2021.

Lamkaddam, H., Dommen, J., Ranjithkumar, A., Gordon, H., Wehrle, G., Krechmer, J., Majluf, F., Salionov, D., Schmale, J., Bjelić, S., Carslaw, K.S., Haddad, I.E., Baltensperger, U., 2021. Large contribution to secondary organic aerosol from isoprene cloud chemistry. Sci. Adv. 7, eabe2952 https://doi.org/10.1126/sciadv.abe2952.

Li, G., Su, H., Ma, N., Tao, J., Kuang, Y., Wang, Q., Hong, J., Zhang, Y., Kuhn, U., Zhang, S., Pan, X., Lu, N., Tang, M., Zheng, G., Wang, Z., Gao, Y., Cheng, P., Xu, W., Zhou, G., Zhao, C., Yuan, B., Shao, M., Ding, A., Zhang, Q., Fu, P., Sun, Y., Pöschl, U., Cheng, Y., 2021. Multiphase chemistry experiment in Fogs and Aerosols in the North China Plain (McFAN): integrated analysis and intensive winter campaign 2018. Faraday Discuss 226, 207–222. https://doi.org/10.1039/D0FD00099J.

Liu, Q., Quan, J., Jia, X., Sun, Z., Li, X., Gao, Y., Liu, Y., 2019. Vertical profiles of aerosol composition over Beijing, China: analysis of in situ aircraft measurements. J. Atmos. Sci. 76, 231–245. https://doi.org/10.1175/JAS-D-18-0157.1.

Liu, T., Clegg, S.L., Abbatt, J.P.D., 2020. Fast oxidation of sulfur dioxide by hydrogen peroxide in deliquesced aerosol particles. Proc. Natl. Acad. Sci. Unit. States Am. 117, 1354–1359. https://doi.org/10.1073/pnas.1916401117.

Lunt, D.J., Chandan, D., Haywood, A.M., Lunt, G.M., Rougier, J.C., Salzmann, U., Schmidt, G.A., Valdes, P.J., 2021. Multi-variate factorisation of numerical simulations. Geosci. Model Dev. (GMD) 14, 4307–4317. https://doi.org/10.5194/gmd-14-4307-2021.

Luo, G., Yu, F., Moch, J.M., 2020. Further improvement of wet process treatments in GEOS-Chem v12.6.0: impact on global distributions of aerosols and aerosol precursors. Geosci. Model Dev. (GMD) 13, 2879–2903. https://doi.org/10.5194/gmd-13-2879-2020.

McNeill, V.F., 2015. Aqueous organic chemistry in the atmosphere: sources and chemical processing of organic aerosols. Environ. Sci. Technol. 49, 1237–1244. https://doi.org/10.1021/es5043707.

Pandis, S.N., Seinfeld, J.H., 1989. Sensitivity analysis of a chemical mechanism for aqueous-phase atmospheric chemistry. J. Geophys. Res. Atmos. 94, 1105–1126. https://doi.org/10.1029/JD094iD01p01105.

Peterson, D.A., Hyer, E.J., Han, S.-O., Crawford, J.H., Park, R.J., Holz, R., Kuehn, R.E., Eloranta, E., Knote, C., Jordan, C.E., Lefer, B.L., 2019. Meteorology influencing

springtime air quality, pollution transport, and visibility in Korea. Elem. Sci. Anth. 7, 57. https://doi.org/10.1525/elementa.395.

Petters, S.S., Cui, T., Zhang, Z., Gold, A., McNeill, V.F., Surratt, J.D., Turpin, B.J., 2021. Organosulfates from dark aqueous reactions of isoprene-derived epoxydiols under cloud and fog conditions: Kinetics, mechanism, and effect of reaction environment on regioselectivity of sulfate addition. ACS Earth Space Chem. 5, 474–486. https://doi.org/10.1021/acsearthspacechem.0c00293.

Plaude, N.O., Stulov, E.A., Parshutkina, I.P., Pavlyukov, Yu.B., Monakhova, N.A., 2012. Precipitation effects on aerosol concentration in the atmospheric surface layer. Russ. Meteorol. Hydrol. 37, 324–331. https://doi.org/10.3103/S1068373912050056.

Rasch, P.J., Barth, M.C., Kiehl, J.T., Schwartz, S.E., Benkovitz, C.M., 2000. A description of the global sulfur cycle and its controlling processes in the National Center for atmospheric Research Community climate model, version 3. J. Geophys. Res. Atmos. 105, 1367–1385. https://doi.org/10.1029/1999JD900777.

Ryu, Y.-H., Min, S.-K., 2022. Improving wet and dry deposition of aerosols in WRF-Chem: updates to below-cloud scavenging and coarse-particle dry deposition. J. Adv. Model. Earth Syst. https://doi.org/10.1029/2021MS002792. In press.

Ryu, Y.-H., Min, S.-K., 2021. Long-term evaluation of atmospheric composition reanalyses from CAMS, TCR-2, and MERRA-2 over South Korea: insights into applications, implications, and limitations. Atmos. Environ. 246, 118062. https://doi.org/10.1016/j.atmosenv.2020.118062.

Ryu, Y.-H., Min, S.-K., Hodzic, A., 2021. Recent decreasing Trends in surface PM2.5 over East Asia in the winter-spring season: different responses to emissions and meteorology between upwind and downwind regions. Aerosol Air Qual. Res. 21, 200654. https://doi.org/10.4209/aaqr.200654.

Scott, B.C., 1982. Theoretical estimates of the scavenging coefficient for soluble aerosol particles as a function of precipitation type, rate and altitude. Atmos. Environ. 16, 1753–1762. https://doi.org/10.1016/0004-6981(82)90268-2 (1967), Precipitation chemistry.

Stein, U., Alpert, P., 1993. Factor separation in numerical simulations. J. Atmos. Sci. 50, 2107–2115. https://doi.org/10.1175/1520-0469(1993)050<2107:FSINS>2.0.CO, 2.

Tai, A.P.K., Mickley, L.J., Jacob, D.J., 2010. Correlations between fine particulate matter (PM2.5) and meteorological variables in the United States: implications for the sensitivity of PM2.5 to climate change. Atmos. Environ. 44, 3976–3984. https://doi.org/10.1016/j.atmosenv.2010.06.060.

Textor, C., Schulz, M., Guibert, S., Kinne, S., Balkanski, Y., Bauer, S., Berntsen, T., Berglen, T., Boucher, O., Chin, M., Dentener, F., Diehl, T., Easter, R., Feichter, H., Fillmore, D., Ghan, S., Ginoux, P., Gong, S., Grini, A., Hendricks, J., Horowitz, L., Huang, P., Isaksen, I., Iversen, I., Kloster, S., Koch, D., Kirkevåg, A., Kristjansson, J. E., Krol, M., Lauer, A., Lamarque, J.F., Liu, X., Montanaro, V., Myhre, G., Penner, J., Pitari, G., Reddy, S., Seland, Ø., Stier, P., Takemura, T., Tie, X., 2006. Analysis and quantification of the diversities of aerosol life cycles within AeroCom. Atmos. Chem. Phys. 6, 1777–1813. https://doi.org/10.5194/acp-6-1777-2006.

Tsui, W.G., Woo, J.L., McNeill, V.F., 2019. Impact of aerosol-cloud cycling on aqueous secondary organic aerosol formation. Atmosphere 10, 666. https://doi.org/10.3390/atmos10110666.

Xu, D., Ge, B., Chen, X., Sun, Y., Cheng, N., Li, M., Pan, X., Ma, Z., Pan, Y., Wang, Z., 2019. Multi-method determination of the below-cloud wet scavenging coefficients of aerosols in Beijing, China. Atmos. Chem. Phys. 19, 15569–15581. https://doi.org/10.5194/acp-19-15569-2019.

Yang, Y., Fu, Y., Lin, Q., Jiang, F., Lian, X., Li, L., Wang, Z., Zhang, G., Bi, X., Wang, X., Sheng, G., 2019. Recent advances in quantifying wet scavenging efficiency of black carbon aerosol. Atmosphere 10, 175. https://doi.org/10.3390/atmos10040175.

Zaveri, R.A., Easter, R.C., Fast, J.D., Peters, L.K., 2008. Model for simulating aerosol interactions and chemistry (MOSAIC). J. Geophys. Res. Atmos. 113 https://doi.org/10.1029/2007JD008782.

Zeng, Y., Wang, M., Zhao, C., Chen, S., Liu, Z., Huang, X., Gao, Y., 2020. WRF-Chem v3.9 simulations of the East Asian dust storm in May 2017: modeling sensitivities to dust emission and dry deposition schemes. Geosci. Model Dev. (GMD) 13, 2125–2147. https://doi.org/10.5194/gmd-13-2125-2020.

Zheng, B., Zhang, Q., Zhang, Y., He, K.B., Wang, K., Zheng, G.J., Duan, F.K., Ma, Y.L., Kimoto, T., 2015. Heterogeneous chemistry: a mechanism missing in current models to explain secondary inorganic aerosol formation during the January 2013 haze episode in North China. Atmos. Chem. Phys. 15, 2031–2049. https://doi.org/10.5194/acp-15-2031-2015.